

ЦРНОГОРСКА АКАДЕМИЈА НАУКА И УМЈЕТНОСТИ  
ГЛАСНИК ОДЈЕЉЕЊА ПРИРОДНИХ НАУКА, 21, 2016.

ЧЕРНОГОРСКАЯ АКАДЕМИЯ НАУК И ИСКУССТВ  
ГЛАСНИК ОТДЕЛЕНИЯ ЕСТЕСТВЕННЫХ НАУК, 21, 2016

THE MONTENEGRIN ACADEMY OF SCIENCES AND ARTS  
PROCEEDINGS OF THE SECTION OF NATURAL SCIENCES, 21, 2016.

UDK 581.116:66.074

*Artan Hoxha\**, *Flamur Bidaj\*\**

## **PREDICTION OF THE REACTION ZONE CHARACTERISTICS AND NO EMISSIONS OF A BURNER OPERATED IN MILD COMBUSTION MODE**

### *Abstract*

An industrial burner operating in the MILD combustion regime with high air preheating and strong internal exhaust gas recirculation is numerically simulated. The burner is characterized by relatively low flame temperatures, low NO<sub>x</sub> emissions, no visible flame and no sound. The ILDM technique is combined with the presumed probability density function approach to simulate turbulent combustion. A computational fluid dynamics (CFD) model is set up comprising the input of geometrical model, mesh-refining process, setting up physical model, handling of algorithms of solution, and the incorporation of appropriate user subroutine that was linked to the fluent code. Predictions of the mean flow field, turbulence kinetic energy, temperature, mass fraction of CO<sub>2</sub>, H<sub>2</sub>O and NO<sub>x</sub> emissions are presented. The calculated mean velocities and temperatures reproduce experimental data reasonably well, but some small discrepancies were found.

The NO emissions calculated are compared both with in-furnace measurements and with the results of a previous study. The distribution of the NO emissions showed the NO peak is just above 95 ppm, and occurs near the maximum temperature region. The maximum of NO emissions occurs between jet of fuel and six jets of air. However, the NO emissions at the exhaust is much smaller, 9.2 ppm.

**Key Words:** MILD combustion; Flameless Burner; CFD

---

\* Artan HOXHA, Polytechnic University of Tirana, Department of Energy, Tirana, Albania

\*\* Flamur BIDAJ, Polytechnic University of Tirana, Department of Energy, Tirana, Albania

## 1. INTRODUCTION

The improvement of combustion efficiency to reduce fossil fuel consumption and reduction of pollutant emissions from practical combustion devices is a key issue in combustion research. A better efficiency is often achieved by air preheating (Wünning and Wünning 1997) [1]. Energy from the exhaust gases is transferred to the combustion air in recuperative or regenerative heat exchangers. Preheating is used in many applications with high temperatures to regain the energy lost by exhaust gases. A negative consequence of air preheating is increased peak flame temperatures with a strong effect on increase of thermal NO formation and NO<sub>x</sub> emissions. Among all the mechanisms (Miller and Bowman, 1989; Hayhurst and Lawrence, 1992) [2], [3], used to form NO the most prominent high temperature process for an oxygen and nitrogen reaction in a combustible air mixture is that of Zeldovich (1946) [4]. For this process, it may be sufficient for the reactants to remain for a few seconds at temperatures of around 1600<sup>0</sup> C and this could be as low as a few milliseconds when temperatures reach 2000<sup>0</sup> C or above (Wünning and Wünning 1997) [1]. These are the typical peak flame temperatures seen when there is preheating, the time duration of residence at points of high temperature is of particular importance. The methods to reduce NO emission are, therefore, based on schemes to reduce either peak flame temperature or the residence time and oxygen concentration in zones with high temperature (Garg, 1994; Wood, 1994) [5], [6]. Different methods have been proposed to reduce NO<sub>x</sub> emissions. These include, exhaust gas recirculation, air staging, reburning and low NO<sub>x</sub> burners. However recent studies, such as Mastorakos et al. (1993)[7], have shown that flue gas recirculation is indeed the most successful scheme to reduce peak flame temperature and NO emission. In the present investigation, instead of mixing inert exhaust gases directly into a flame, flue gases are introduced upstream as a third component and dilute the fresh fuel/air mixture. Such a combustion regime needs the reactants to be preheated above the self-ignition temperature and enough inert combustion products to be entrained in the reaction region. Characteristic features of this combustion mode are low flame temperatures, no emission of sound, no visible flame, and barely any NO formation. This combustion regime was referred to as flameless oxidation by Wunning and Wunning (1997) [1], and further insight into this combustion technique was recently given by de Joannon et al. (1999) [8], where it is referred to as MILD combustion. The term in the present paper used is moderate or intense low oxygen dilution (MILD) combustion. All these aspects make MILD combustion worthy of further investigations. Several studies have been devoted to understanding its operational conditions (Cavigiolo et al. 2003) [9] and its mechanisms and critical parameters (de Joannon et al. 2005) [10]. The MILD combustion technology has been successfully applied in several

industries (Wünning, 2003) [11], that require a high and homogeneous temperature distribution within the combustion chamber e. g., in the glass and ceramic industry, in steel thermal treatments. These burners are usually designed to operate both in flame and in MILD mode by varying the reactants feeding mode. The combination of recuperative MILD combustion burners with radiant tubes is a widely applied solution in many thermal treatments of material surfaces, to avoid any contact or contamination of the flue gases with the stock surface to be treated. Implementation has been impeded by a lack of fundamental understanding of the establishment and detailed structure of this combustion regime. Few fundamental studies have been performed to look at the detailed structure of this regime (Dally et al. 2002; Ahn et al. 2003; Medwell et al. 2007) [12, 13, 14]. Choi and Katsuki (2001) [15] investigated the feasibility of flameless oxidation in industrial glass furnaces. They found that the combustion process was sustained even with low-calorific-value fuels and low oxygen concentrations if the combustion air was preheated above the fuel self-ignition temperature. Results also showed that NO<sub>x</sub> formation was controlled by the mixing process between fuel and the preheated air. The application of MILD combustion in different fields than thermal treatment processes is also very attractive. The advantages of a clean and quiet combustion process could be exploited in several fields of application, including power generation, micro cogeneration, and low-temperature applications. Wang et al. (2006) [16] performed a technical, environmental, and economic analysis of NO<sub>x</sub> reduction technologies at a gas turbine power station. Results showed that the use of recuperative MILD combustion burners could offer an effective method for reducing NO<sub>x</sub> emissions, the technology being much cheaper than SCR and requiring only a slight increase in capital cost and electricity selling price with respect to the simple cycle gas turbine power plants. Recently, the industrial interest has increased attention not only to the experimental characterization of MILD combustion burners, but also to their modeling through computational fluid dynamics (CFD). In particular, CFD may be of great help in the area of optimization of burners performances by investigating geometrical details, such as injection nozzles, configurations and internal devices for flue gas recirculation. Actually, despite the flame homogeneity and smooth gradients occurring in this combustion mode, MILD combustion appears more difficult to model than conventional flames, e. g., premixed or diffusion flames, because the high dilution levels and the relatively low temperatures lower the chemical reaction rates, making them comparable to turbulent mixing phenomena, which are enhanced by recirculation. Therefore the turbulence–chemistry interaction treatment becomes a crucial point in the modeling procedure. Orsino et al. (2001) [17] investigated the performance of three combustion models for predicting the combustion of natural gas with high-temperature air and large

quantities of flue gas and found that all models failed in the vicinity of the fuel injection. However, the authors claimed that they could obtain excellent NO predictions through the steady flamelet library. Christo and Dally (2005) [18] investigated numerically a jet in hot co-flow burner replicating MILD combustion regime. The burner was characterized experimentally by Dally et al. (2004) [19]. The authors used different turbulence, combustion, and kinetic models, comparing their performance. In particular they showed that mixture fraction/probability density function and flamelet approaches perform poorly for the MILD combustion regime. The eddy dissipation model also gave unsatisfactory results. Better predictions were achieved through combustion models considering both chemistry and turbulence effects.

A combustion chamber operating in the mild combustion mode was investigated experimentally by Plessing et al. (1998) [20]. Instantaneous temperatures and OH-radical fields were measured optically, along with NO<sub>x</sub> emissions. It was found that mild combustion takes place in the well stirred reactor regime, and that maximum local temperatures were below 1,650 K. The OH concentration in the combustion zone was lower than in non-preheated undiluted turbulent premixed flames. The NO<sub>x</sub> emissions decreased when switching from the stable flame mode to the mild combustion regime, where they were only around 10 ppm. Additional measurements consisting of LDA measurements of mean and fluctuating velocity components along several transverse profiles, residence times and new instantaneous temperature and OH images in the same combustor have been recently made by Özdemir and Peters (2001) [21] include. Coelho and Peters (2001) [22] simulated a furnace operating in the MILD combustion mode by applying the flamelet approach to describe turbulence/chemistry interactions. They compared predictions with measurements supplied by Plessing et al. (1998) [20] and Özdemir and Peters (2001) [21]. Although a qualitative agreement between the experimental and predicted flow field was observed, some considerable discrepancies were present. In addition, the residence time was underestimated by the numerical model, and the flamelet approach was found to be unable of describing correctly the NO formation. Better results could be achieved by means of the unsteady flamelets (Dally et al. 2004) [19]. The present work presents a numerical simulation of this combustor based on a combined PDF/ turbulent flow model, where an ILDM model for detailed chemical reaction is used and to validate the predictions using the recently acquired experimental data. This model provides a realistic description of turbulent flame in our combustion chamber. Detailed kinetics in most cases is computationally prohibitive for turbulent reactive three-dimensional flows (Pope, 1991) [23]. This is caused by the large number of chemical species sometimes more than 1000, which react in several thousand reactions, e. g., in low-temperature oxidation of higher hydrocarbons

(Chevalier, 1993) [24]. To decrease the computational effort, several methods for the reduction of the detailed chemical mechanisms have been devised (Smook, 1991; Peters and Rogg, 1993) [25], [26]. One of these techniques is the method of intrinsic low dimensional manifolds (ILDM) (Maas and Pope, 1992; Maas and Pope, 1993) [27], [28]. In the present paper, ILDM table has 43 species and 393 reactions. Turbulence/chemistry interactions are described by applying a presumed PDF (probability density function) model. The proposed numerical model contains one subroutine that was linked to the fluent code. Combustor under investigation is presented, followed high accuracy computational grid (3745552 cells and 3789720 grid points) especially near the holes by the results obtained from the simulation and the paper ends with a summary of the main conclusions.

## 2. MATERIALS AND METHODS

### 2.1 Burner

The burner is a REKUMAT-Mild Combustion Burner with a built-in heat exchanger for air preheating with a nominal power of 5400 W (Plessing et al. 1998). It is rectangular parallelepipedal in shape with  $250 \times 250 \text{ mm}^2$  cross-section, 485 mm length and both the burner and the exhaust are placed at the bottom of the combustor.

The burner consisted of a central nozzle of 4.7 mm diameter conically-elevated 25 mm from the six peripheral nozzles of 5 mm diameter located 40. Özdemir and Peters (2001) [21] detailed these operations. Dimensions are given

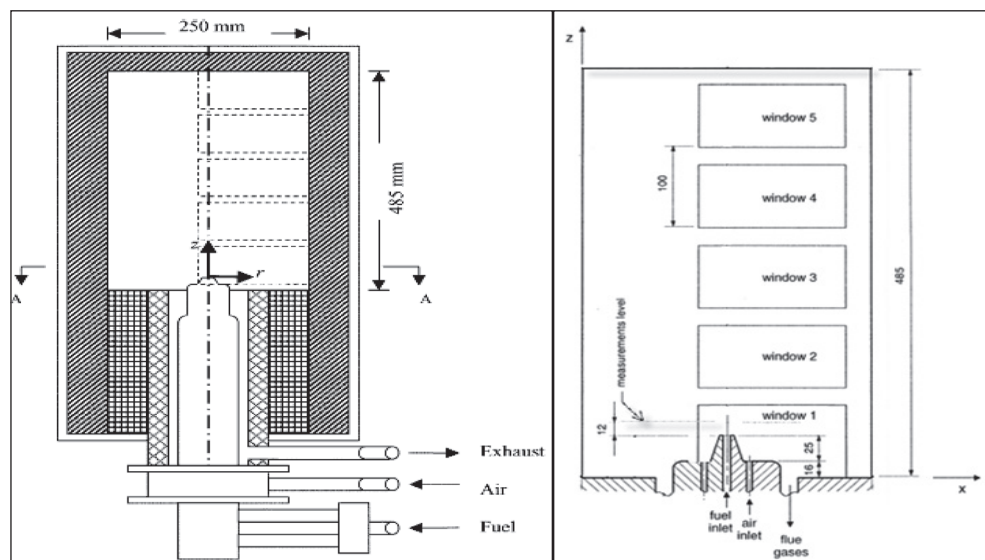


Figure 1. The Burner

in Figure. 1. The fuel was methane ( $\text{CH}_4$ ) and was run at 5400 W with an overall equivalence ratio of unity (Özdemir and Peters, 2001)[21]. The corresponding mass flow rates for air and fuel are 6.5 kg/h and 0.38 kg/h. In the present investigation, burner runs in the non-premixed mode where the six peripheral nozzles supplied only air and the fuel was introduced from the central nozzle whereas in premixed combustion the central nozzle was unused with the air and the fuel mixture being introduced peripherally. The exhaust gases preheat the combustion air in a heat exchanger and the inlet air temperature was obtained from the estimated efficiency of the heat exchanger and was calculated as 650 K. The same temperature was assumed for the fuel at the fuel nozzle exit. The wall temperature was around 1040 °C and the temperature of the exhaust gases after exchanging heat with the incoming components was around 680 °C (Özdemir and Peters, 2001)[21]. Measurements to the combustor were made by five windows as in Fig. 1.

## 2.2 Numerical solution procedure

The use of numerical simulations was shown to be a very important research instrument in combustion (Warnatz et al. 2001) [29]. The numerical solution procedure is split into two parts. The solution of the flow and the mixing field is performed in a Computational Fluid Dynamics (CFD) code, where version 6.3.26, 3 ddp of the fluent code was used, but the combustion models available in fluent were not activated. An appropriate user subroutine was linked to the fluent code based on a combined PDF/ turbulent flow model, where an ILDM model for detailed chemical reaction is used. In the ILDM code, ILDM table are built. In the Fluent code the Favre averaged form of the conservation equations for mass and momentum are solved. Turbulence is modeled by using the standard  $k$ - $\epsilon$  turbulence model, which involves the solution of transport equations for the turbulent kinetic energy, and for its dissipation rate. Standard values are used for all the constants of the model. In addition, equations for the mean mixture fraction  $\xi$ , its variance  $\xi_v$  and the mean enthalpy are solved.

The NO emissions are calculated in a post-processing stage.

## 2.3 ILDM chemistry

The ILDM method is used to reduce the system dynamics in the composition space to lower dimensional manifolds. This manifold approximates an invariant system manifold of slow motions. Automatically Reduced Reaction Mechanisms – ILDM Chemistry is a dynamical approach, in contrast to the conventional approaches, tries to find out the directions in which the source term vector will rapidly reach a steady-state (Maas and Pope 1992; Maas and Pope, 1993)[27], [28]. ILDM is a vector defined as the zeroth level-set of a multidimensional function.

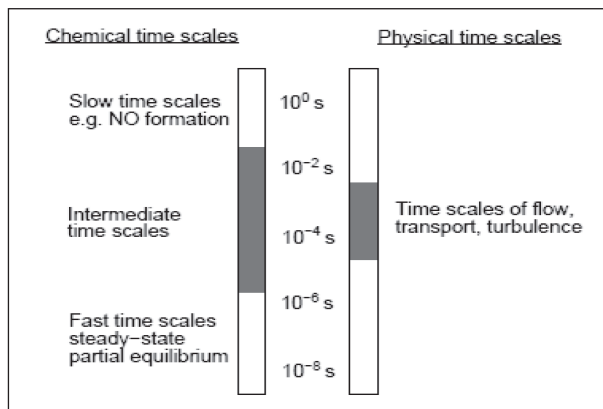


Figure 2. Time scales in a typical combustion processes (Warnatz et al. 2001) [29].

The chemical processes faster than the turbulent mixing time scales are assumed to be in dynamic equilibrium with the mixing processes and the slower chemical processes (Figure. 2). This allows the fast processes to be expressed as combinations of slow processes, entailing considerable reduction in number of variables required to describe chemistry. The manifolds have a property to attract reaction trajectories.

Reaction paths in the detailed mechanism will proceed to the manifold rapidly, while the subsequent movement on the manifold will be slow. The progress variables parameterize this slow movement on the manifold. For discrete values of the progress variables, compositions are calculated and stored in a data base.

For a detailed chemical mechanism with  $n_s$  species,  $n_s$  different time scales govern the process. If  $n_f$  time scales are assumed to be in equilibrium, the system can be described in only  $n_r = n_s - n_f$  degrees of freedom. An assumption that all the time scales are relaxed results in assuming complete equilibrium. Here, the only variables required to describe the chemical system is the mixture composition (its mixture fraction), the pressure and the mixture enthalpy (or temperature). This results in a zero-dimensional manifold. An assumption that all but  $n_r$  time scales are relaxed leads to a system that is described by the mixture fraction, the pressure, the temperature and  $n_r$  other parameters called progress variables. In addition to reducing the number of transport equations that need to be solved, this also reduces the dimension of the pdf that the reaction rate needs to be integrated over in turbulent flows.

Figure. 3 shows the reaction trajectories for a stoichiometric  $\text{CH}_4$ -air system, projected on the  $\text{H}_2\text{O}$ - $\text{CO}_2$  plane. The equilibrium point is marked by a circle. Complete trajectories till equilibrium are shown in the first diagram. Each trajectory is for a distinct initial condition. The system takes approximately 5 ms to

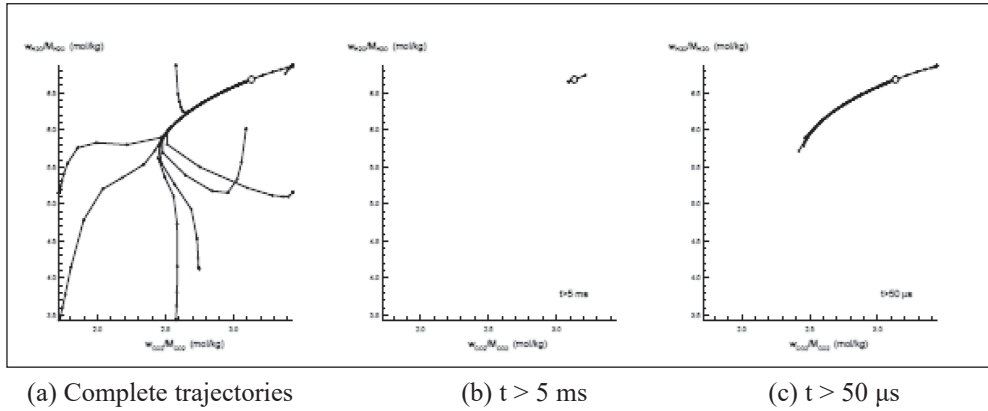


Figure 3. Trajectories in a methane-air system.  
 ◦ denotes the equilibrium (Warnatz et al. 2001).

reach equilibrium, as shown in the third diagram. After a time of  $50 \mu s$ , a single line in the state space corresponding to one dimensional manifold is seen. All processes slower than  $50 \mu s$  are described by the movement along this line. All processes faster than  $50 \mu s$  are assumed to be in equilibrium. Higher dimensional manifolds are required to filter out processes which are faster than  $50 \mu s$ . If however, all processes are to be slower than  $5$  ms, we would only see the trajectory as a point, corresponding to all processes being in equilibrium.

## 2.4 Mathematical treatment of ILDM

In the ILDM method, the fast chemical reactions do not need to be identified *a priori*. An eigenvalue analysis of the detailed chemical mechanism needs to be carried out which identifies the fast processes in dynamic equilibrium with the slow processes. A homogeneous, adiabatic, isobaric system is determined by  $n = n_s + 2$  variables ( $n_s$  species, the pressure and the temperature). The state of the system is given as a point, in an  $n$ -dimensional state space. The governing equation system can be written as

$$\frac{\partial \vec{\psi}}{\partial t} = \vec{F}(\vec{\psi}) \quad (1)$$

with  $\vec{\psi} = (T, p, Y_1, Y_2, \dots, Y_{n_s})^T$ . Since, this equation system is, in general, non-linear, the function can be linearized locally at a point by a Taylor series approximation

$$\frac{\partial \vec{\psi}}{\partial t} = \vec{F}(\vec{\psi}_0) + J(\vec{\psi} - \vec{\psi}_0) \quad (2)$$

Then, the low-dimensional manifold is defined as the set of points in the state space for which

$$Q_L^T J = 0 \quad (3)$$

where  $Q_L^T$  is the matrix obtained from  $Q^T$  by omitting the first  $2 + n_c + n_r$  rows,  $n_c$  being the number of elements, namely the rows corresponding to the conserved and slowly changing variables (pressure, enthalpy and element composition).

In the present investigation, the detailed chemical mechanism for methane combustion consisted of 43 species (see Table 1) and 393 elementary reactions. For atmospheric pressure flames, two progress variables; mass fractions of  $\text{CO}_2$  and  $\text{H}_2\text{O}$  ( $Y_{\text{CO}_2}$  and  $Y_{\text{H}_2\text{O}}$ ) are shown enough to represent chemistry in sufficient detail (Warnatz et al., 2001)[29]. For the discrete values of the progress variables shown in Table 2, compositions were calculated for 1 bar pressure and stored in the ILDM table. Some data from the ILDM table at constant temperature and mixture fraction are shown in Figure 1.

Table 1. Species involved in chemical kinetics.

H	$\text{H}_2$	$\text{O}_2$	OH	$\text{H}_2\text{O}$	O	$\text{HO}_2$	$\text{H}_2\text{O}_2$
$\text{CO}_2$	CO	$\text{CH}_4$	$\text{CH}_3$	$3\text{CH}_2$	$1\text{CH}_2$	CH	$\text{CH}_3\text{OH}$
$\text{CH}_3\text{O}$	$\text{CH}_2\text{OH}$	$\text{CH}_2\text{O}$	CHO	$\text{CH}_3\text{O}_2\text{H}$	$\text{CH}_3\text{O}_2$	$\text{C}_2\text{H}_6$	$\text{C}_2\text{H}_5$
$\text{C}_2\text{H}_4$	$\text{C}_2\text{H}_3$	$\text{C}_2\text{H}_2$	$\text{C}_2\text{H}$	HCCO	$\text{CH}_2\text{CO}$	$\text{CH}_2\text{CHO}$	$\text{CH}_3\text{CHO}$
$\text{CH}_3\text{CO}$	$\text{C}_3\text{H}_2$	$\text{C}_3\text{H}_3$	$\text{C}_3\text{H}_4$	$\text{C}_3\text{H}_5$	$\text{C}_3\text{H}_6$	$\text{N-C}_3\text{H}_7$	$\text{N-C}_4\text{H}_9$
$\text{C}_6\text{H}_6$	$\text{N-C}_7\text{H}_{16}$	$\text{N}_2$					

Table 2. Matrix of discrete values of progress variables.

	<i>Min.</i>	<i>Max.</i>	<i>Step</i>
Temperature	300	3000	50
Mixture fraction	0	1	0.005
Mass Fraction of $\text{CO}_2$	0	1	0.005
Mass Fraction of $\text{H}_2\text{O}$	0	1	0.005

## 2.5 Pdf formulation with ILDM

In this case is assumed presumed pdf method and the shape of the pdf is assumed to be, beta function. Two progress variables,  $\text{CO}_2$  and  $\text{H}_2\text{O}$  are used for creating the ILDM table. Using two progress variables compared to a single progress variable allows a better resolution of time scales in cases when the gap between the physical and chemical time scales is narrow. The instantaneous rate

of reaction of the progress variables  $\dot{Y}_{CO_2}^C$  and  $\dot{Y}_{H_2O}^C$  is obtained from a query to the ILDM table. The Favre-averaged species equation contains the mean chemical source terms. The source terms therefore need to be integrated over the probability density function. The average reaction rates are obtained by averaging the laminar rates from the ILDM tables using the probability density functions.

For the case of the reaction progress variable  $CO_2$ , a transport equation needs to be solved, given as:

$$\frac{\partial \bar{\rho} \widetilde{Y_{CO_2}}}{\partial t} + \nabla \cdot (\bar{\rho} \widetilde{\vec{u}} \widetilde{Y_{CO_2}}) = \nabla \cdot (\bar{\rho} D_T \widetilde{\vec{u}} \nabla \widetilde{Y_{CO_2}}) + \bar{\rho} \widetilde{Y_{CO_2}^C} \quad (4)$$

The instantaneous source term due to chemistry ( $\dot{Y}_{CO_2}^C$ ) is obtained from ILDM and this needs to then be integrated over a probability density function in order to get the mean chemical source term.

$$\widetilde{Y_{CO_2}^C} = \int \dot{Y}_{CO_2}^C(\xi, T, Y_{CO_2}) \bar{P}(\xi, T, Y_{CO_2}) d\xi dT d(Y_{CO_2}) \quad (5)$$

In the case of two progress variables, where  $H_2O$  is the second progress variable, the transport equation for  $H_2O$  is given as

$$\frac{\partial \bar{\rho} \widetilde{Y_{H_2O}}}{\partial t} + \nabla \cdot (\bar{\rho} \widetilde{\vec{u}} \widetilde{Y_{H_2O}}) = \nabla \cdot (\bar{\rho} D_T \widetilde{\vec{u}} \nabla \widetilde{Y_{H_2O}}) + \bar{\rho} \widetilde{Y_{H_2O}^C} \quad (6)$$

while the PDF for  $H_2O$  is given as follows

$$\widetilde{Y_{H_2O}^C} = \int \dot{Y}_{H_2O}^C(\xi, T, Y_{H_2O}) \bar{P}(\xi, T, Y_{H_2O}) d\xi dT d(Y_{H_2O}) \quad (7)$$

As mentioned above a detailed reaction mechanism consisting of 43 species and 393 elementary reactions is used to produce ILDM tables with two reaction progress variables. The ILDM table is a 4-dimensional table for the two-progress-variable case. All other species compositions, enthalpy, density and specific heat are functions of these defining dimensions.

The fluent code applied in the present investigation helps the user to call user-defined-subroutine written by the user to extend the capabilities of the original software. It is possible to call a user-defined-subroutine before the main loop for the iterative solution of the governing differential equations is initiated. This allows the input of tabulated data or any kind of preliminary calculations specific to the problem under consideration. At all the iterations, selecting the equations to be solved, and solving other transport equations not available in fluent is possible. In the last case source terms are provided in user defined-subroutine. In the present work, the mean and the variance of the mixture fraction, the enthalpy, mass fraction of  $CO_2$ , mass fraction of  $H_2O$ , transport equations have been solved

in this way. Before the end of every iteration, a user-defined-subroutine is called to adjust the results of the calculations. This allows, for example, the temperature and density computed by Fluent to be, ignored and replaced by those computed according to the code provided by the user. In summary, Fluent is basically used for pre-processing and post-processing operations, and for the numerical solution of the equations of mass and momentum conservation, and turbulent quantities. All the calculations related to the combustion model are provided by our own code which is linked to the original fluent software.

### 3. RESULTS AND DISCUSSION

For better results, calculations are done in the whole burner. Geometry is successfully created by using a preprocessor code called Rhinoceros. The volume discretization (meshing) is realized into finite elements called „cells”, which will be the fundamental parts of the future calculations, because all of the equations will be solved for each one of these elements. The grid is created in preprocessor code, ANSYS ICEM CFD, based on geometry, holes of the air and the methan (O-grid). In ICEM code is created structured grid with blocking strategy and mesh. The meshing is very fine near the holes for better results. The grid has 3.745.552 cells and 3.789.720 grid nodes. Hexahedral type of elements is used as they offer better results. Once the discretization of the geometric volume is completed, the mesh is totally exported, into the main code (processor), fluent. Figure

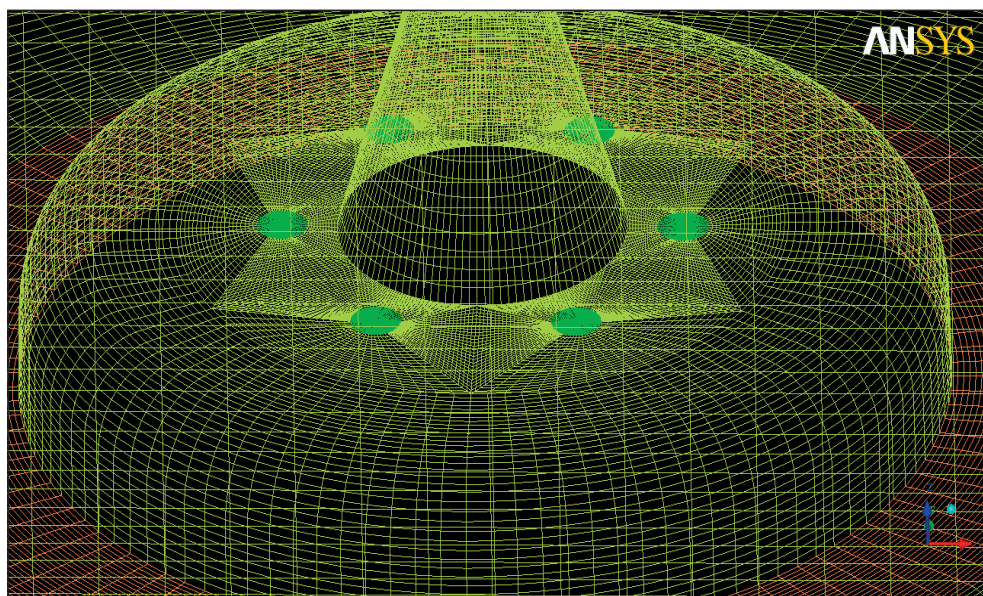


Figure 4. Mesh of the burner

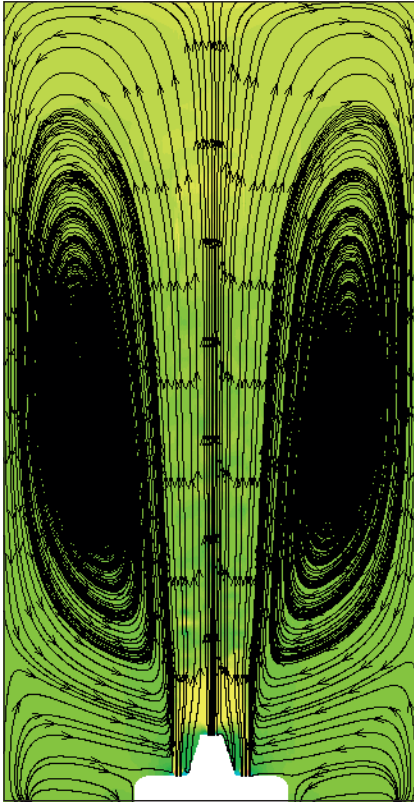


Figure 5. Velocity streamlines

4 depicts part of the results corresponding to the aforementioned meshing process of the burner.

In the following figures are shown some preliminary results. The full results after the flow is stabilized (flow has converged and the level of accuracy is very high) are presented in another paper.

The streamlines field at a vertical plane crossing the axis of the burner ( $y = 0$ ) is shown in Figure 5. The air and the fuel enter the combustor, flow to the top of the furnace while combustion is taking place, impinge on the top section, deflect towards the side walls and return to the bottom. Part of the combustion gases mix with the incoming air, and are internally recirculated, while the remaining combustion gases leave the furnace through the bottom exhaust.

The predicted and measured velocity components in the  $x$  and  $z$  directions denoted by  $u$  and  $w$  are depicted in figure 6 respectively, at five different heights  $z = 12.5, 112.5, 212.5, 312.5$  and  $412.5$  mm. In

addition to the results computed with Fluent, those obtained by the measurements (Özdemir, Peters, 2001) [21] are also displayed in the figure. The results presented below were obtained by first computing the flow field with ILDM library. In the first window both the fuel and air jets are clearly apparent in the predictions, but only the air jet appears in the measurements, because no measurements are available at the center of the combustor. At large distances from the center, large positive values velocities were replaced with small velocities of the reverse flow. At a slightly higher distance from the burner the flow patterns of the fuel and five peripheral air jets quickly combined in to a single jet. The predictions reproduce with small discrepancies, the measured profiles, apart from the region in the vicinity of the axis, in window 2, where the predictions still show evidence of the individual jets. Figure 6b depicts the outward momentum of the peripheral air jets opposed at large radial distances by the exhaust gases driven back to the vicinity of the burner. Therefore, low velocity values predominate in this region. On the other hand, the inward spreading of the air jets is prohibited around the centerline by the flow set by fuel jet so that small radial velocities ap-

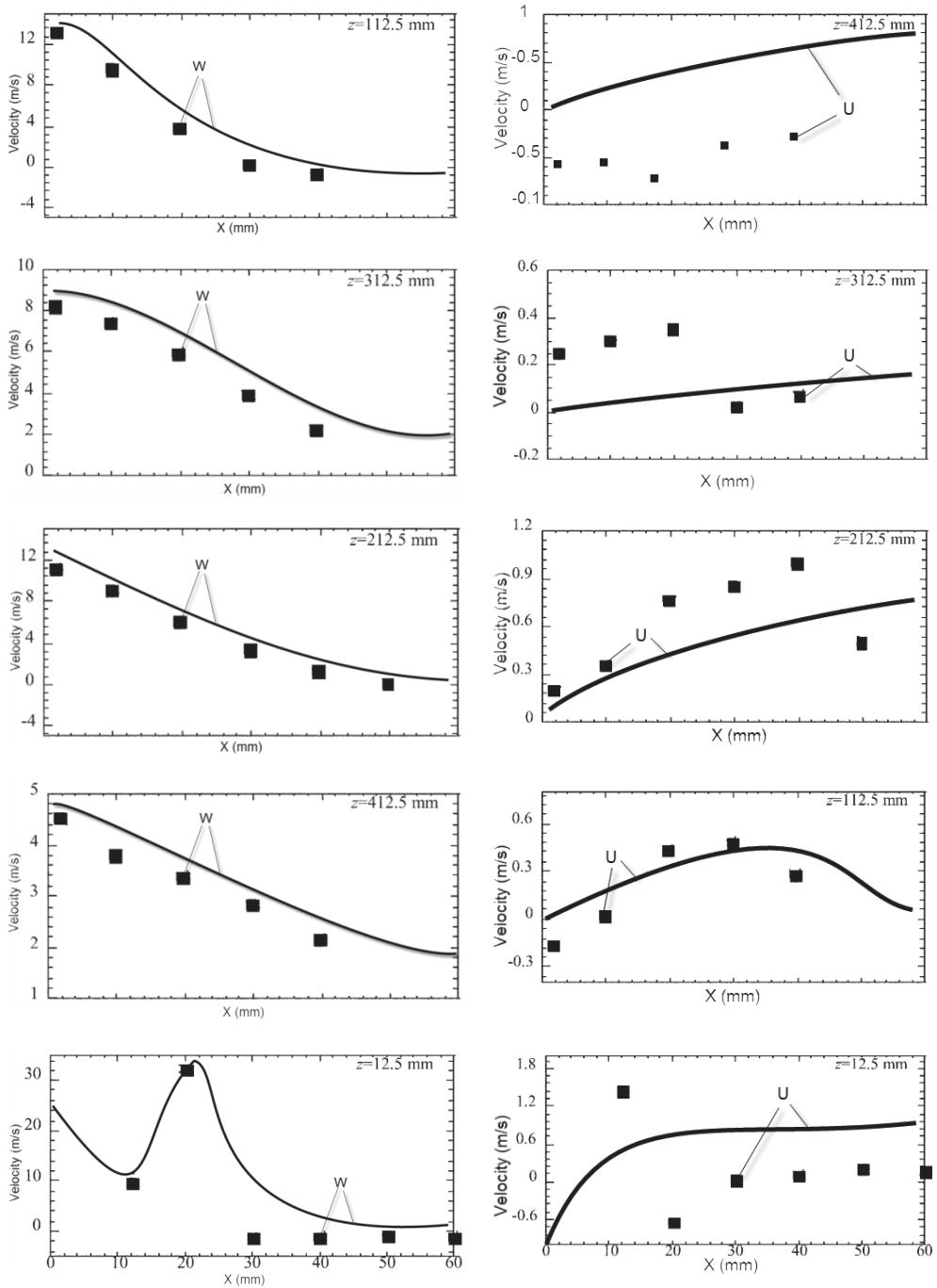


Figure 6. a, b. Predicted and measured profiles of mean velocity: a-w component; b-u component (symbols, measurements; solid lines, Fluent predictions).

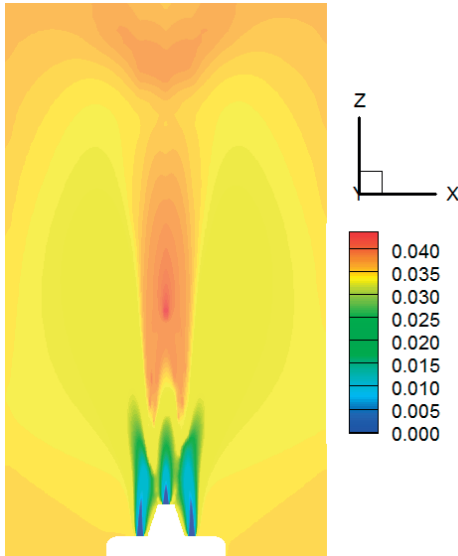


Figure 7. Predicted mass fraction of  $H_2O$  contours

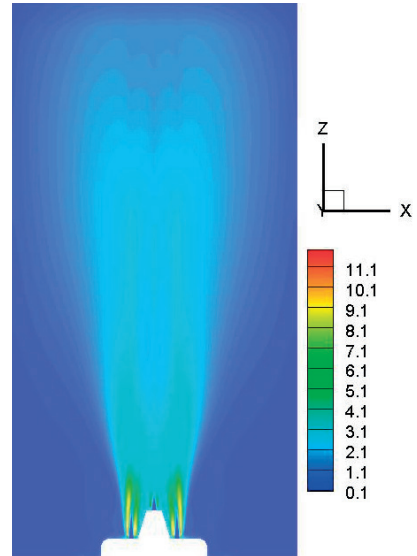


Figure 8 Predicted turbulent kinetic energy contours

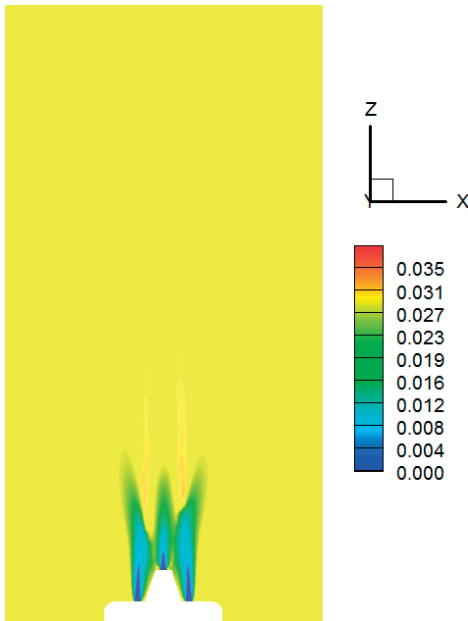


Figure 9. Predicted mass fraction of  $CO_2$  contours

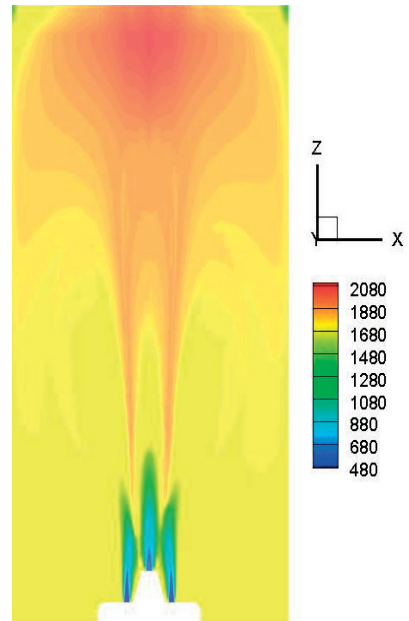


Figure 10. Contours of the predicted temperature field

peared to be confined between fuel jet and the wall. The influence of the fuel jet decreased as the distance along the burner axis decreased and disappeared completely when the heat release due to the progress of the chemical reaction become

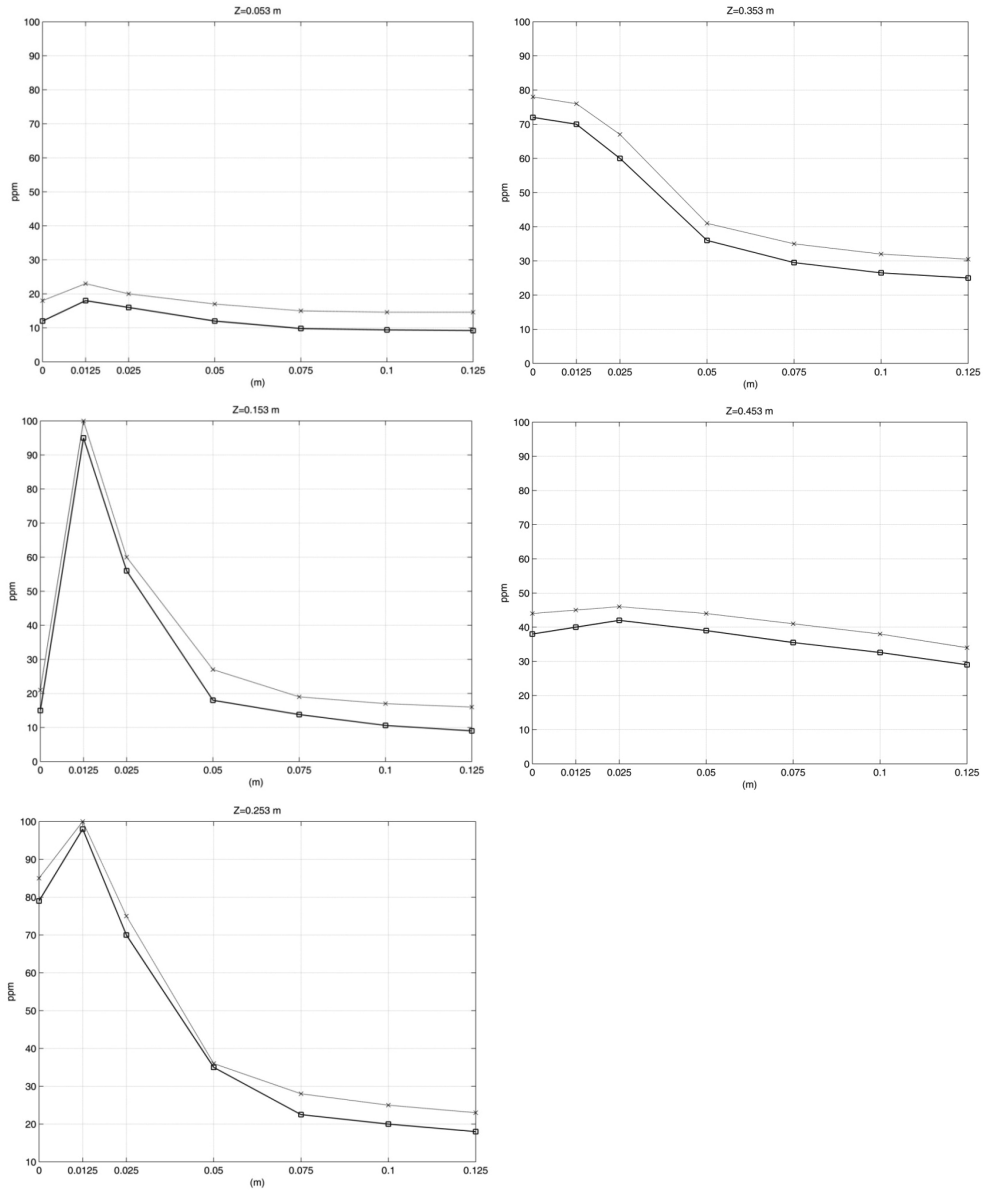


Figure 11. NO Emissions [ppm] in different elevations on the burner

- 1- Solid line – NO Emissions on the burner
- 2- Dashed line – NO Emissions according to Co&Pe

dominant. Radial momentum (x-direction) at these axial locations (z-direction), which seemed relatively small compared to the axial momentum, was generated by the thermal expansion of the hot gases rather than the spreading of the jets. At the upper windows the velocity component,  $w$ , is consistently over predicted.

This may be related to corresponding errors in the temperature field, but the lack of temperature data prevents a more detailed analysis.

In the other windows the predicted profiles reproduce the data reasonably well, but some small discrepancies in the window 2, 3 and especially on the top of the burner were found. Figure 7, 8, 9 shows mass fraction of  $\text{CO}_2$ , mass fraction of  $\text{H}_2\text{O}$  and turbulent kinetic energy. Contours of the predicted temperature field are depicted in figure 10. The maximum temperature is slightly above 1,900 K and occurs at the top of the burner at the level of window 5. The temperature range in the furnace is quite narrow compared with most currently used furnaces. The experimental temperature Rayleigh images (Özdemir, Peters, 2001) [21] do not allow a comparison with the predictions, since only a few images of the instantaneous temperature field are available for  $\phi = 1$ . The images are not similar to those presented in (Özdemir, Peters, 2001)[21] in all the burner and especially in window 5 where temperature in general in this part is higher because the flame is not stabilized in this zone.

The predicted NO emissions are shown in figure 11. The distribution of the NO emissions showed the NO peak is just above 95 ppm, and occurs near the maximum temperature region. The maximum of NO emissions occurs between jet of fuel and six jets of air. However, the NO emissions at the exhaust is much smaller. Measured values in the exhaust of the combustor were 4-10 ppm. As a comparison, the predicted NO emissions in the same burner and for the same equivalence ratio, but for somewhat different operating conditions, were about 9.2 ppm.

#### 4. CONCLUSION

A combustor operating in the mild combustion mode was numerically simulated using the Fluent code (Ansys Fluent). Version 6.3.26, 3 ddp of the fluent code was used, but the combustion models available in Fluent were not activated. An appropriate user subroutine was linked to the Fluent code based on a combined PDF/ turbulent flow model, where an ILDM model for detailed chemical reaction is used. In the ILDM code, ILDM table are built. Calculations are done in the whole burner. The grid has 3.745.552 cells and 3.789.720 grid nodes and was very fine near the holes of air and fuel. Very fine and structured grid and using PDF with ILDM has given better results. Predictions of the mean velocity calculated by the code were compared with experimental data. It was found that flow field prediction reproduce the measurements, but some small discrepancies were found in the mean velocity components.

Contours of the predicted temperature field were found and are compared with experimental data. There are some small discrepancies on the five windows and especially on the top of the burner, on window 5, because of the flame was not fully stabilized. Also the predicted field of enthalpy, turbulent kinetic energy,

dissipation rate, mixture fraction, mixture fraction variance, mass fraction of  $\text{CO}_2$ , mass fraction of  $\text{H}_2\text{O}$  were found.

The distribution of the NO emissions showed the NO peak is just above 95 ppm, and occurs near the maximum temperature region. The NO emissions at the exhaust is much smaller, about 9.2 ppm and measured values in the exhaust of the combustor were 4-10 ppm.

### ACKNOWLEDGEMENTS

The authors thank Prof. Dr. İ. Bedii Özdemir, Head of Fluids Group at Istanbul Technical University for his assistance and technical support in all stages of this project.

Computing resources used in this work were provided by the National Center for High Performance Computing of Turkey (UYBHM) under grant number 001352011.

### REFERENCES

- [1] Wüning JA, Wüning JG. 1997. „Flameless oxidation to reduce thermal NO-formation”. *Progress in Energy and Combustion Science* 23; 81-94
- [2] Miller JA, Bowman CT. 1989. „Mechanism and modeling of nitrogen chemistry in combustion”. *Progress in Energy and Combustion Science* 15; 287-338
- [3] Hayhurst AN, Lawrence AD. 1992. „Emissions of nitrous oxide from combustion sources”. *Progress in Energy and Combustion Science* 18; 529-552
- [4] Zeldovich J. 1946. „The oxidation of nitrogen in combustion and explosions”. *Acta Physiochim URSS XXI* (4)
- [5] Garg A. 1994. „Specify better low- $\text{NO}_x$  burners for furnaces”. *Chemical Engineering Progress*. January, 46-49
- [6] Wood SC. 1994. „Select the right  $\text{NO}_x$  control technology”. *Chemical Engineering Progress* January: 32-38
- [7] Mastorakos E, Taylor AM, Whitelaw JH. 1993. „Turbulent counterflow flames with reactants diluted by hot products”. *Joint Meeting of the British and German Sections. The Combustion Institute, Cambridge. Mediterranean Combustion Symposium*, pp. 347–360.
- [8] de Joannon M, Langella G, Beretta F, Cavaliere A, and Noviello C. 1999. *Proc. of Mediterranean Combustion Symposium*, pp. 347–360.
- [9] Cavigiolo A, Galbiati MA, Effuggi A, Gelosa D, Rota R. 2003. „Mild combustion in a laboratory-scale apparatus”. *Combustion Science and Technology*. 175; 1347–1367.
- [10] de Joannon M, Cavaliere A, Faravelli T, Ranzi E, Sabia P, Tregrossi A. 2005. „Analysis of process parameters for steady operations in methane mild combustion technology”. *Proceedings of the Combustion Institute* 30; 2605–2612.
- [11] Wüning J. G. 2003. „FLOX®-Flameless Combustion” *Thermprocess Symposium, WS Wärmeprozessstechnik GmbH*
- [12] Dally B. B, Karpets A. N, Barlow R. S. 2002. „Structure of turbulent non-premixed jet flames in a diluted hot coflow”. *Proceedings of the Combustion Institute* 29; 1147–1154.
- [13] Ahn C, Akamatsu F, Katsuki M, Kitajima A. 2003. *The Fourth Asia-Pacific Conference on Combustion*. pp. 40–43.

- [14] 14. Medwell P. R, Kalt P. A. M, Dally B. B. 2007. „Simultaneous imaging of OH, formaldehyde, and temperature of turbulent nonpremixed jet flames in a heated and diluted coflow”, *Combustion and Flame* 148; 48–61.
- [15] 15. Choi G. M, Katsuki M. 2001. „Advanced low NOx combustion using highly preheated air” *Energy Conversion and Management* 42; 639–652
- [16] Wang Y. D, Huang Y, McIlveen-Wright D, McMullan J, Hewitt N, Eames P, Rezvani S. 2006. „A techno-economic analysis of the application of continuous staged-combustion and flameless oxidation to the combustor design in gas turbines. *Fuel Processing Technology* 87; 727–736
- [17] Orsino S, Weber R, Bolletini U. 2001. „Numerical simulation of combustion of natural gas with high-temperature air”. *Combustion Science and Technology* 170; 1–34.
- [18] Christo F. C, Dally B. B. 2005. „Modeling turbulent reacting jets issuing into a hot and diluted coflow”. *Combustion and Flame* 142; 117–129.
- [19] Dally B. B, Riesmeier E, Peters N. 2004. „Effect of fuel mixture on moderate and intense low oxygen dilution combustion”. *Combustion and Flame* 137; 418–431.
- [20] Plessing T, Peters N, Wüning J. G. 1998. Twenty-Seventh Symposium (Int.) on Combustion, *The Combustion Institute, Pittsburgh, PA*, pp. 3197–3204.
- [21] Özdemir B, Peters N. 2001. „Characteristics of the reaction zone in a combustor operating at MILD combustion”. *Experiments in Fluids* 30; 683–695
- [22] Coelho P. J, Peters N. 2001. „Numerical simulation of a mild combustion burner. *Combustion and Flame* 124; 503–518.
- [23] Pope S. B, 1991. „Computations of turbulent combustion” *Progress and challenges. Symposium (International) on Combustion. Proceedings of the Combustion Institute, Volume 23; 591–612*
- [24] Chevalier C, 1993. „Entwicklung eines detaillierten Reaktionsmechanismus zur Modellierung der Verbrennungsprozesse von Kohlenwasserstoffen bei Hoch- und Niedertemperaturbedingungen,” *Ph. D. thesis, Institut für Technische Verbrennung, Universität Stuttgart*,
- [25] Smooke M. D, (ed.), 1991. „Reduced Kinetic Mechanisms and Asymptotic Approximations for Methane-Air Flames”, *Lecture Notes in Physics 384, Springer, Berlin*,
- [26] Peters N, Rogg B. 1993. „Reduced Kinetic Mechanisms for Applications in Combustion Systems”, *Springer, Berlin*,
- [27] Maas U, Pope S. B. 1992. „Simplifying chemical kinetics: Intrinsic low-dimensional manifolds in composition space”. *Combustion and Flame* 88; 239–264
- [28] Maas U, Pope S. B. 1993. „Implementation of simplified chemical kinetics based on intrinsic low-dimensional manifolds”. *Proceedings of the Combustion Institute. Symposium (International) on Combustion, Volume 24, Issue 1, 1992, Pages 103–112*
- [29] Warnatz J, Maas U, Dibble RW. 2001. *Combustion, 3rd ed; Springer, Heidelberg, Germany*.